



**HAL**  
open science

## Toxicity of palytoxin, purified ovatoxin-a, ovatoxin-d and extracts of *Ostreopsis cf. ovata* on the Caco-2 intestinal barrier model

Marin-Pierre Gemin, Rachelle Lanceleur, Lisa Meslier, Fabienne Herve, Damien Reveillon, Zouher Amzil, Eva Ternon, Olivier Thomas, Valérie Fessard

### ► To cite this version:

Marin-Pierre Gemin, Rachelle Lanceleur, Lisa Meslier, Fabienne Herve, Damien Reveillon, et al.. Toxicity of palytoxin, purified ovatoxin-a, ovatoxin-d and extracts of *Ostreopsis cf. ovata* on the Caco-2 intestinal barrier model. *Environmental Toxicology and Pharmacology*, 2022, 94, pp.103909. 10.1016/j.etap.2022.103909 . anses-03701528

**HAL Id: anses-03701528**

**<https://anses.hal.science/anses-03701528>**

Submitted on 22 Jul 2024

**HAL** is a multi-disciplinary open access archive for the deposit and dissemination of scientific research documents, whether they are published or not. The documents may come from teaching and research institutions in France or abroad, or from public or private research centers.

L'archive ouverte pluridisciplinaire **HAL**, est destinée au dépôt et à la diffusion de documents scientifiques de niveau recherche, publiés ou non, émanant des établissements d'enseignement et de recherche français ou étrangers, des laboratoires publics ou privés.

Copyright

# Toxicity of palytoxin, purified ovatoxin-a, ovatoxin-d and extracts of *Ostreopsis cf. ovata* on the Caco-2 intestinal barrier model

GEMIN Marin-Pierre<sup>1\*</sup>, LANCELEUR Rachelle<sup>2\*1</sup>, MESLIER Lisa<sup>2</sup>, HERVE Fabienne<sup>1</sup>, REVEILLON Damien<sup>1</sup>, AMZIL Zouher<sup>1</sup>, TERNON Eva<sup>3</sup>, THOMAS P. Olivier<sup>4</sup>, FESSARD Valérie<sup>2</sup>

1 IFREMER, Phycotoxins Laboratory, F-44311 Nantes, France

2 ANSES, Fougères Laboratory, Toxicology of Contaminants Unit, French Agency for Food, Environmental and Occupational Health & Safety, Fougères 35306, France

3 Sorbonne Université, CNRS, Laboratoire d'Océanographie de Villefranche, UMR 7093, BP 28, F-06230 Villefranche-sur-Mer, France

4 Marine Biodiscovery, School of Chemistry and Ryan Institute, National University of Ireland Galway, University Road, H91TK33 Galway, Ireland

## Corresponding author:

Valérie FESSARD

Anses Laboratoire de Fougères

Unité de Toxicologie des contaminants

10 B rue Claude Bourgelat,

35306 Fougères cedex, FRANCE

Tel: +33 (0)2 99 94 66 85

E-mail: [Valerie.fessard@anses.fr](mailto:Valerie.fessard@anses.fr)

---

\*co-first authors

## Abstract

Human intoxications in the Mediterranean Sea have been linked to blooms of the dinoflagellate *Ostreopsis cf. ovata*, producer of palytoxin (PITX)-like toxins called ovatoxins (OVTXs). Exposure routes include only inhalation and contact, although PITX-poisoning by seafood has been described in tropical regions. To address the impact of OVTXs on the intestinal barrier, dinoflagellate extracts, purified OVTX-a and -d and PITX were tested on differentiated Caco-2 cells. Viability, inflammatory response and barrier integrity were recorded after 24h treatment. OVTX-a and -d were not cytotoxic up to 20 ng/mL but increased IL-8 release, although to a lesser extent compared to PITX. While PITX and OVTX-a (at 0.5 and 5 ng/mL respectively) affected intestinal barrier integrity OVTX-d up to 5 ng/mL did not. Overall, OVTX-d was shown to be less toxic than OVTX-a and PITX. Therefore, oral exposure to OVTX-a and -d could provoked lower acute toxicity than PITX.

Keywords: palytoxin; ovatoxins; toxicity; permeability; purification; inflammation

## 1 Introduction

Since 2005, blooms of the dinoflagellate *Ostreopsis cf. ovata* have been involved in human health hazards along the Western Mediterranean coasts especially in Italy, France and Spain (Vila et al., 2016). Reported symptoms include eye and nose irritation, rhinorrhea and general malaise. The toxins thought to be responsible for such health disorders are called ovatoxins (OVTXs). They are analogs of the well-known toxin, palytoxin (PITX). Several analogs of OVTXs (from -a to -l) have been identified in *Ostreopsis* species (Brissard et al., 2015; Ciminiello et al., 2010; Ciminiello et al., 2012b; García-Altare et al., 2015; Tartaglione et al., 2017; Tartaglione et al., 2016). Generally, OVTX-a is the

major analog produced by the Mediterranean strains of *O. cf. ovata* (Brissard et al., 2014; Gémin et al., 2020; Soliño et al., 2020; Tartaglione et al., 2017). Moreover, OVTX-a is also the only one for which the structure has been elucidated by Nuclear Magnetic Resonance (NMR) (Ciminiello et al., 2012a; Ciminiello et al., 2012c), while the structures of the other OVTXs have been only proposed from data obtained by high resolution mass spectrometry (Figure 1).

Irritations due to aerosol exposure as well as dermal and ocular contacts have been reported along the Mediterranean coasts (Kermarec et al., 2008; Tubaro et al., 2011; Vila et al., 2016). No human intoxication has been declared so far from Mediterranean seafood, although the presence of PITX-like compounds has been reported in fish and shellfish of several Mediterranean countries (Aligizaki et al., 2008; Amzil et al., 2012; Biré et al., 2015).

Human poisoning through inhalation and dermal/ocular contact has been well demonstrated for PITX, especially due to the manipulation of aquarium containing the zoantharians *Palythoa* and *Zoanthus* corals (Calon et al., 2019; Farooq et al., 2017; Hall et al., 2015; Schulz et al., 2019; Tubaro et al., 2011; Wonneberger et al., 2020). Illness by consumption of seafood contaminated with PITX has also been reported in the tropical and sub-tropical areas with various clinical effects involving mainly neurological and gastrointestinal disturbances (Tubaro et al., 2011). Moreover, several cases of intoxications have been listed in domestic animals (cats and dogs) (Bates et al., 2020).

*In vivo* toxicity of PITX through different routes of exposure is also well documented. Following intravenous and intraperitoneal (ip) administration, the onset of symptoms is very rapid, and death occurs within few minutes (Patocka et al., 2018). A Lethal Dose 50% (LD<sub>50</sub>) value (0.68 µg/kg) after ip in mice has been measured recently (Boente-Juncal et al., 2020b). Conversely, PITX is far less toxic by gavage with a LD<sub>50</sub> around 600 µg/kg in mice (Boente-Juncal et al., 2020b; Patocka et al., 2018). Fever, ataxia, drowsiness and weakness of limbs, followed by death have been observed after oral exposure of animals. Adverse effects on the gastro-intestinal tract such as swelling of the cavities and abdominal hemorrhage as well as abdominal pains have been recently observed after PITX oral

administration (Boente-Juncal et al., 2020b). Moreover, the lowest dose that did not induce an effect was estimated at 15 µg/kg. A recent study on chronic oral exposure up to 28 days in mice reported that no macroscopic effect could be detected with a daily dose of with 0.03 µg/kg PITX (Boente-Juncal et al., 2020a). However, abdominal swelling was observed at higher doses (0.1, 1 and 3.5 µg/kg). *In vitro*, PITX is known to alter normal ion homeostasis and the ubiquitous Na<sup>+</sup>/K<sup>+</sup> ATPase of the plasma membrane is one of its molecular target (Habermann, 1989; Satoh et al., 2003; Wu, 2009). Nevertheless, some differences have recently been highlighted about the Na<sup>+</sup>/K<sup>+</sup>-ATPase isoforms. Indeed, a high expression of the β2 isoform has been linked with a higher sensitivity of monocytes to PITX (Pelin et al., 2020).

Unlike for PITX, data on the toxicity of OVTXs are scarce. This lack of information is mainly due to the difficulty to access purified OVTXs. Pure OVTX-a was tested for toxicity by ip injection in mice showing that a dose of 7 µg/kg induced the death after 30 min (Ciminiello et al., 2012d). This first study depicted that OVTX-a was largely less toxic than PITX. However, more recently, only a slight difference of toxicity between OVTXs and PITX after ip administration to rats was observed: a LD<sub>50</sub> of 3.3 µg/kg was obtained with a purified mixture of OVTXs isolated from a Japanese *O. cf. ovata* strain (containing mostly OVTX-a but also OVTX-d and -e) compared to a LD<sub>50</sub> value of 1.8 µg/kg with PITX (Poli et al., 2018).

Additional data about the OVTXs toxicity on the intestinal barrier are missing to better understand the events following their ingestion. Indeed, *in vitro* toxicity results with OVTXs are rather limited. A study on HaCaT keratinocytes concluded that purified OVTX-a was 100-fold less potent to induce cytotoxicity (IC<sub>50</sub> = 1.1 µM) than PITX (IC<sub>50</sub> = 0.018 µM) (Pelin et al., 2016b). In contrast, PITX has been documented to be cytotoxic to both non-differentiated and differentiated human intestinal Caco-2 cells (Fernández et al., 2013; Pelin et al., 2012; Valverde et al., 2008).

In this study, we investigated the *in vitro* effects of crude extracts of two Mediterranean *O. cf. ovata* strains as well as two purified OVTX analogs (OVTX-a and -d) on differentiated Caco-2 cells. The

impacts on viability, inflammatory response and intestinal barrier integrity were recorded and the responses to OVTX-a and -d were compared with PITX.

## 2 Material and methods

### 2.1 Chemicals

Cell culture products were purchased from Gibco (Cergy-Pontoise, France). Bovine serum albumin (BSA), Tween 20, TritonX100, 3-[4,5-dimethylthiazol-2-yl]-2,5 diphenyl tetrazolium bromide (MTT), lucifer yellow and HEPES were supplied by Sigma-Aldrich (Saint Quentin Fallavier, France). Monoclonal interleukin 8 (IL-8), biotinylated monoclonal IL-8 antibodies, SuperBlock blocking buffer, streptavidin peroxidase, Tumor Necrosis Factor alpha (TNF $\alpha$ ) and 3,3',5,5'-tetramethylbenzidine (TMB) were purchased from ThermoFisher Scientific (Waltham, MA). Palytoxin (HPLC purity = 85.8%) was purchased from Wako (Wako Pure Chemical Industries, Ltd., Japan). Acetonitrile (ACN) and methanol (MeOH) of LC-MS grade (Chromasolv) were supplied by Honeywell (Saint-Germain-en-Laye, France) while dimethylsulfoxide (DMSO, SeccoSolv<sup>®</sup>) was from Merck. Milli-Q water was obtained from a Milli-Q integral 3 system (Merck Millipore, Molsheim, France). Acetic acid (> 99.8%, HiPerSolv CHROMANORM) and Sephadex<sup>™</sup> LH-20 (GE Healthcare) were purchased from VWR (Strasbourg, France).

### 2.2 *Ostreopsis* cultures

Two strains of *Ostreopsis* cf. *ovata* were obtained from the Mediterranean Culture Collection of Villefranche-sur-Mer: MCCV54 and MCCV55. Cells were cultivated in Fernbach Duran<sup>®</sup> flasks (VWR, Strasbourg, France) containing 500 mL of L1 medium without silicate (Guillard, 1975) with 0.2% of soil extract (Séchet et al., 2012) at salinity 38. Cultures were maintained at 27 °C, with an irradiance of 300  $\mu\text{mol m}^{-2} \text{s}^{-1}$  and under a 14:10 h light:dark cycle. Cells were harvested in the stationary phase after 21 days of growth by filtration on a 11  $\mu\text{m}$  sieve (Plastique-TAMIS Nylon DIN4197 w: 11  $\mu\text{m}$ ,

Mougel, Nantes, France), centrifuged (2000 g, 10 min, room temperature) to remove remaining water, then stored at -20 °C. In total, 35 g of cell pellets were obtained from 35 L of cultures of the strain MCCV55 for the purification of OVTXs. Additionally, two cultures of MCCV54 and MCCV55 were performed to compare the activity of crude extracts, as they displayed two different toxin profiles (Table 1).

## ***2.3 Toxin extraction and purification***

### ***2.3.1 Crude extracts***

Cell pellets were extracted with a mixture MeOH/H<sub>2</sub>O (1:1 v/v) using a ratio of 4 mL per gram of wet pellet. The mixture was vortexed for 1 min at 2500 rpm, then centrifuged (5 min, 4000 g, 4 °C) and finally the supernatant was recovered. This extraction was repeated twice, and the supernatants were pooled. The resulting extracts were stored 48 h at -20 °C, then centrifuged (20 min, 4000 g, 4 °C) to remove cell debris. Finally, they were concentrated under a nitrogen flow (N-evap, Organomation) at 30 °C.

### ***2.3.2 Fractionation by size exclusion chromatography***

Ovatoxin-a and -d were purified from the strain MCCV55 as the toxin profile was less complex (Table 1). The concentrated crude extracts (i.e. 1.2 mL corresponding to 10 g of biomass) were first fractionated by size exclusion chromatography (Sephadex™ LH-20) in a glass chromatographic column (70 × 1.5 cm; 30 g of resin conditioned in MeOH 100 %) as in Brissard et al. (2015). Finally, 30 fractions of 10 mL were recovered after elution with MeOH and OVTXs eluted between 32 and 61% of the total volume of the column (ca. 40 to 80 mL). The presence of OVTXs in the fractions was ascertained by liquid chromatography coupled to tandem mass spectrometry (LC-MS/MS).

### ***2.3.3 Purification of OVTX-a and -d from MCCV55***

The purification of OVTX-a and -d was performed in two consecutive steps by semi-preparative chromatography (LC-UV with an Uptisphere C<sub>18</sub>-TF column (250 mm x 10 mm, 5 µm, Interchim)), as in Brissard et al. (2015) with minor modifications.

Solvent A was water/acetic acid (100:0.2, v/v) and solvent B was acetonitrile/water/acetic acid (95:5:0.2, v/v/v) while the flow rate was 4 mL/min. First, a 'fast' gradient was used to collect all OVTXs in one fraction (ca. 10 mL): 20 to 100% of solvent B in 30 min, maintained 5 min at 100%, 100 to 20% in 5 min and finally maintained 5 min at 20%. The injection volume was 500 µL and the mix of OVTXs was collected between 11 and 13 min of elution. Then, the gradient was adjusted to separate OVTX-a, -d and -e : 30 to 33% of solvent B in 35 min, 33 to 90% in 1 min, maintained 5 min, 90 to 30% in 1 min and finally maintained 5 min at 30%. The volume of injection was 50 µL. Fractions containing only OVTX-d (first eluted peak between 21.0 and 22.5 min) and OVTX-a (last peak, between 25.5 and 28.0 min) were finally concentrated at 30 °C and dissolved in 1 mL of DMSO (Figure S1).

#### 2.3.4 Quantification of OVTXs by LC-MS/MS

Crude extracts and purified OVTX-a and -d were dissolved in 1 mL DMSO prior to toxicity assessment and quantified as PITX equivalent (PITX eq.) by LC-MS/MS as in Gémin et al. (2020). Samples were diluted by addition of MeOH (MeOH/DMSO, 80:20, v/v) before LC-MS/MS analyses. The standard of palytoxin initially solubilized in MeOH 100% was diluted accordingly to avoid any change in the ionization due to the charge stripping phenomenon (Hahne et al., 2013).

#### 2.4 Caco-2 cell culture

Caco-2 cells (HTB-37), obtained from the American Type Culture Collection (ATCC) (Manassas, VA), were maintained in Minimum Essential Medium containing 5.5 mM D-glucose, Earle's salts and 2 mM L-alanyl-glutamine (MEM GlutaMAX) supplemented with 10% fetal bovine serum (FBS), 1% non-essential amino acids, 50 IU/mL penicillin and 50 µg/mL streptomycin at 37 °C and 5% CO<sub>2</sub>. Cells were used at passages 29 to 42. A vehicle control (2 and 2.5% DMSO for cytotoxicity/inflammation and transport respectively) was included in each experiment.

Caco-2 cells were seeded at 200 000 cells/ml in 96 well plates for cytotoxicity and IL-8 release and in 12 well plates on PET inserts of 0.4 µm for monolayer integrity assays. The medium was renewed every 2 to 3 days. At 25 days post-seeding, the differentiated cells were used for toxin treatment.



The cell treatments with extracts and toxins were done in FBS-free medium in order to increase the sensitivity and to limit the interferences. Table S1 presents the amount of toxin for each concentration used for cell treatment in various units to facilitate comparisons.

## 2.5 MTT assay

Following a 24 h treatment with the extracts or toxins, the cells were incubated at 37 °C for 2 h with 100 µL of 500 µg/mL MTT solution prepared in medium. After removal of the medium from the wells which were kept for IL-8 detection (see below), 100 µL/well of DMSO was added to solubilize the mitochondrial dye. The plates were gently shaken for 5 min and the absorbance was recorded with a FLUOstar Optima microplate reader (BMG Labtek, Champigny sur Marne, France) at 570 nm. The cytotoxicity level was calculated compared to the value for the solvent control fixed to 100% cell survival.

## 2.6 IL-8 release

At the end of the 24 h treatment, the cell medium from each well of the 96-well plates used for the MTT assay was collected. The levels IL-8 released were measured using an enzyme-linked immunosorbent assay (ELISA). Primary IL-8 antibody (M801), biotin-conjugated human IL-8 (M802B), recombinant IL-8 cytokine, SuperBlock blocking buffer, TMB, Tween 20, sulfuric acid and streptavidin horseradish peroxidase (HRP) were obtained from Thermofisher Scientific. Tumor Necrosis Factor alpha (TNF $\alpha$ ), Thermofisher Scientific) (100 ng/mL) was used as positive control. Following 24 h incubation with the extracts and toxins, the cell media were collected and frozen at -20 °C until analysis. Ninety six well plates (Nunc maxisorp) were coated with IL-8 primary antibody (M801) at 1 µg/mL and incubated overnight at 4 °C. Between each step, wells were washed 3 times with Phosphate Buffer Saline (PBS)-Tween 20 (0.05%). After saturation with SuperBlock for 1 h, samples and standards (IL-8 recombinant) were added into the wells and incubated at room temperature for 1.5 h. Biotin-conjugated human IL-8 antibodies (0.1 µg/mL) were then added followed by 100 µL of HRP 1:1000 labeling. Finally, 50 µL of the chromogenic substrate TMB was added and the reaction was stopped

with sulfuric acid (2 M). Plates were read at 405 nm. The concentrations of IL-8 expressed in pg/mL were calculated against a standard curve prepared in duplicate. Four independent experiments with two technical replicates per experiment were performed.

## 2.7 Monolayer integrity assays

### 2.7.1 TEER measurement

The trans-epithelial electrical resistance (TEER) of the Caco-2 cultures was measured to evaluate the monolayer integrity before and after 4 and 24 h treatments with extracts or toxins loaded in the apical compartment. The TEER measurements and analysis were performed as previously described (Reale et al., 2020) except that Lucifer Yellow (LY) exposure was limited to 2 h only. Two to four independent experiments were performed.

### 2.7.2 LY crossing

After toxin treatment, the ability of LY to cross the Caco-2 cultures was determined as previously described (Reale et al., 2020) to evaluate monolayer integrity. The amount of LY in the basal compartment was expressed relative to that of the amount loaded in the apical compartment, and then expressed per hour. Two to three independent experiments were performed.

## 2.8 Statistics

GraphPad Prism software was used for statistical analyses. An analysis of variance (ANOVA) was performed, and, when the effect of concentration was significant ( $P < 0.05$ ), the values were compared to the control using the Dunnett's test.

# 3 Results

## 3.1 MCCV54 and 55 extracts content

The two strains of *O. cf. ovata* MCCV54 and 55 showed two different OVTX profiles by LC-MS/MS, although they were isolated from the same bloom event from the bay of Villefranche-sur-Mer, France (Jauzein et al., 2017). Indeed, 5 OVTX analogues (OVTX-a, -b, -c, -d and -e) were detected in

MCCV54 while only 3 analogues (OVTX-a, -d and -e) were noticed in MCCV55 (Table 1). Both strains produced OVTX-a as the major analog (around 58 and 89% of the total OVTX for MCCV54 and MCCV55, respectively). It should be noted that OVTX-b and -c were below the LOD in the crude extract of the strain MCCV55.

Table 1: Concentration (ng PLTX eq./mL) and relative content (%) of ovatoxins (OVTXs) in the crude extracts of strain MCCV54 and 55.

		Iso-PITX	OVTX-a	OVTX-b	OVTX-c	OVTX-d	OVTX-e	OVTX-f	Total
<b>MCCV54 extract</b>	ng PITX eq./mL	< LOD	4 900	2 700	180	320	250	< LOD	8 300
	%	-	58	33	2.2	3.8	3	-	100
<b>MCCV55 extract</b>	ng PITX eq./mL	< LOD	18 000	< LOD	< LOD	900	1 200	< LOD	20 000
	%	-	89	-	-	4.5	6.2	-	100

## 3.2 Purified ovatoxins

The extraction and purification process yielded 223 µg of OVTX-a and 10.5 µg of OVTX-d, corresponding to a yield of purification of 2.2 and 1.5% respectively. The level of purity could not be determined precisely but the TIC (Total Ion Chromatogram, Figure S2) showed that each OVTX solution contained only one analogue and was referred to as OVTX-a and OVTX-d.

## 3.3 Differentiated Caco-2 cells viability (MTT assay)

### 3.3.1 *Ostreopsis* crude extracts

Both crude extracts of *O. cf. ovata* (strains MCCV54 and MCCV55), induced cytotoxicity in differentiated Caco-2 cells, with MCCV54 extract being slightly less cytotoxic than the MCCV55 one (Figure 2): IC<sub>50</sub> was 45.23 ng PITX eq./mL with a 95% confidence interval ranging from 34.77 to 58.84ng PITX eq./mL for the MCCV54 extract and 33.53 ng PITX eq./mL with a 95% confidence interval ranging from 27.00 to 41.65 ng PITX eq./mL for the MCCV55 extract.

### 3.3.2 Palytoxin and ovatoxins

Cytotoxicity on differentiated Caco-2 cells with PITX reached about 50% at the highest concentration (200 ng/mL). No effect on differentiated Caco-2 cells was observed for both OVTX-a and -d up to 20 ng/mL (Figure 3). It was not possible to test higher concentrations of OVTX-a and -d due to solvent toxicity.

## 3.4 Inflammatory response

### 3.4.1 *Ostreopsis* crude extracts

Both crude extracts of *O. cf. ovata* (strains MCCV54 and MCCV55) induced an increase of IL-8 release even at the lowest concentrations tested (0.65 and 1.56 ng PITX eq./mL respectively) (Figure 4). However, the increase was statistically significant only for MCCV55 at 1.56 and 3.13 ng PITX eq./mL. A decrease of IL-8 release was observed with the intermediate concentrations followed by the absence of response with the highest concentrations, likely due to cytotoxicity.

### 3.4.2 Palytoxin and ovatoxins

The release of IL-8 after 24 h of PITX treatment reached a maximum at concentrations between 3.13 and 12.5 ng/mL (Figure 5) with a statistically significant increase. The decrease observed with higher concentrations is likely due to toxicity induced by PITX on the Caco-2 monolayer.

The inflammatory response of OVTX-a and -d increased gradually with a statistical significance at 5 ng/mL for OVTX-a and with lower concentrations at 1.25 and 2.5 ng/mL for OVTX-d (Figure 5). The response decreased gradually with higher concentrations although no cytotoxicity was noticed up to 20 ng/mL for both analogs.

## 3.5 Caco-2 monolayer integrity

### 3.5.1 *Ostreopsis* crude extracts

We did not observe any alteration of the Caco-2 monolayer integrity after 4 and 24 h with the extract from the MCCV54 strain (Figures 6A and 7A). In contrast, the MCCV55 extract affected slightly the intestinal barrier integrity but only after 24 h exposure at the highest concentration tested (0.5 ng/mL): although no significant decrease of TEER was observed (Figure 6B), a slight increase of LY crossing, although not significant, (Figure 7B) was detected.

### 3.5.2 Palytoxin and ovatoxins

PITX affected the intestinal integrity at the highest concentration (0.5 ng/mL) mostly after 24 h treatment even a slight effect was already observed after 4h treatment (Figures 8A and 9A). Although, OVTX-a did not induce any alteration of the monolayer integrity after 4 h treatment, it decreased TEER and increased LY crossing at the highest concentration (5 ng/mL) after 24 h treatment (Figures 8B and 9B). TEER was also significantly decreased at 24h with 0.25 ng/mL PITX and 2.5 ng/mL OVTX-a but without any significant increase of LY Papp. No effect on intestinal barrier integrity was observed even after 24 h exposure with OVTX-d up to 5 ng/mL (Figures 8C and 9C).

The main results obtained during this work are compiled in Table2. It showed that the concentrations of both *O. cf ovata* extracts and purified toxins inducing cytotoxicity on differentiated Caco2 cells could vary according to support used for running experiments (96 well plates or inserts). Apart from that, the results were consistent when comparing the responses induced by *O. cf ovata* extracts and the different toxins.

Table 2: Resume of the main results obtained after 24h treatment on differentiated Caco2 cells on 96 well plates (MTT and IL8) or on inserts (TEER and Papp LY)

	MTT	IL8	TEER	Papp LY
<b>MCCV54</b>	IC50 = 45.23 ng PITX eq./mL	Maximum at 1.3 ng PITX eq./mL	No effect up to 0.48 ng PITX eq./mL	No effect up to 0.48 ng PITX eq./mL
<b>MCCV55</b>	IC50 = 33.53 ng PITX eq./mL	Maximum at 3.13 ng PITX eq./mL	No effect up to 1.21 ng PITX eq./mL	Increase at 1.21 ng PITX eq./mL
<b>PITX</b>	IC50 around 200 ng/mL	Maximum at 6.25 ng/mL	Decrease at 0.25 and 0.5 ng/mL	Increase at 0.5 ng/mL
<b>OVTX-a</b>	No toxicity up to 20 ng/mL	Maximum at 5 ng/mL	Decrease at 2.5 and 5 ng/mL	Increase at 5 ng/mL
<b>OVTX-d</b>	No toxicity up to 20 ng/mL	Maximum at 1.25 ng/mL	No effect up to 5 ng/mL	No effect up to 5 ng/mL

## 4 Discussion

The LC-MS/MS toxin profiles of both *O. cf. ovata* strains MCCV54 and MCCV55 were similar to the two main OVTX profiles observed in strains from the Mediterranean area (Brissard et al., 2014; Crinelli et al., 2012; Guerrini et al., 2010; Soliño et al., 2020; Tartaglione et al., 2017), corresponding to the profiles 1 and 2 described by Tartaglione et al. (2017), that contain OVTX-a to -e or OVTX-a, -d, -c respectively.

The first purification of OVTX-a (700 µg from 80 L of culture of the strain OOAN0816) (Ciminiello et al., 2012d) was less challenging compared to the MCCV54 strain with a 6 times higher yield, probably due to the absence of OVTX-b (12% instead of 2.2%, Table S2). However, evaporation can also affect the yield as reported previously (Brissard et al., 2015). In the present study, even though evaporation to dryness was avoided, significant losses were still noted after a long evaporation (i.e. between 3 and 15 days) at 30 °C under nitrogen flow (Table S2). Thus, we recommend to use a minimal volume of solvent and to reduce as much as possible the duration of the evaporation or to test other techniques for evaporation. Moreover, it has been also suggested that storage even at -20 °C can lead to important losses that may result from adsorption to silanols of the glass and/or transformation of OVTXs (Brissard et al., 2015).

The crude extracts of both *O. cf. ovata* strains were toxic to differentiated Caco-2 cells, although MCCV55 showed a higher toxicity (around 2-fold) compared to MCCV54, likely due to a higher level of total toxins (20 000 and 8 600 ng PITX eq./mL respectively) and a higher percentage of OVTX-a (89 and 58% respectively) in MCCV55 compared to MCCV54. Consistently, only the MCCV55 crude extract affected the Caco-2 monolayer integrity. A difference of toxicity was also shown with the same *O. cf. ovata* strains in the bioassay on *Artemia franciscana*, although the highest toxicity for MCCV55 could not be only due to the highest level of PITX equivalent (Pavaux et al., 2020). However, an inflammatory response was observed with both extracts, with a similar level of IL-8 released for both strains.

We could not detect cytotoxicity on differentiated Caco-2 cells after 24 h treatment with OVTX-a and -d at concentrations up to 20 ng/mL. In fact, PITX did not show any cytotoxic effect also at 20 ng/ml but some cytotoxicity was detected above 100 ng/mL, with an IC<sub>50</sub> of approximately 200 ng/mL (or 75 nM). The few data available in the literature concluded to a lower potency of OVTX-a compared to PITX in the hemolytic test (10 fold) and in the MTT assay (100 fold) on HaCaT keratinocytes (Pelin et al., 2016b). Unfortunately, from our MTT assay on differentiated Caco-2 cells, higher concentrations of pure OVTXs could not be tested due to solvent toxicity (maximum 2% DMSO for the top concentration 20 ng/mL). If our results are consistent with the literature reporting cytotoxicity of PITX on Caco-2 cells, some discrepancies exist when looking at the level of response. In fact, a 50% decrease of cell metabolism was observed beyond 3.6 ng/mL (1.35 nM) PITX after 24 h exposure on differentiated Caco-2 cells (Fernández et al., 2013). The difference of sensitivity, observed also for the permeability results (see below), can be explained by different Caco-2 cellular features. On non-differentiated Caco-2 cells, an IC<sub>50</sub> of 0.26 ng/mL (0.1 nM) has been reported after a 24 h treatment with PITX (Valverde et al., 2008), although a higher potency was even described by Pelin et al (2012) with an IC<sub>50</sub> of 0.024 ng/mL (8.9 pM) after 4 h exposure. The toxicity of PITX on Caco-2 cells has been reported to be due to a necrotic effect, which can be followed by an apoptotic response (Valverde et al., 2008). The toxin induces the disruption of F-actin cytoskeleton that can affect cell adherence

(Louzao et al., 2008; Valverde et al., 2008) and, consequently, cell monolayer integrity. Injuries of the gastro-intestinal tissues including erosion of small intestinal villi at the top and sticky mucus secretion were observed shortly after a sublingual administration of PITX to mice, although these changes became unclear after 8 h (Ito and Yasumoto, 2009). A repeated sublingual exposure to PITX led to more severe injuries in stomach and intestine with exfoliation of epithelial cells and naked lamina propria (Ito and Yasumoto, 2009). Nevertheless, it was shown that PITX was less toxic through intragastric and intrarectal routes compared to intravenous, intratracheal or intraperitoneal administrations (Wiles et al., 1974).

While low or no effect on intestinal permeability was observed after only 4 h treatment with the three toxins, a significant decrease was induced after 24 h with PITX at 0.5 ng/mL (0.19 nM) and with OVTX-a at 5 ng/mL (1.89 nM). Therefore, we showed that OVTX-a was slightly less toxic (10 fold) than PITX and that OVTX-d was even less toxic than OVTX-a for this endpoint. A difference of *in vitro* toxicity between OVTX-a and PITX was already pointed out, although with a higher order of magnitude (100 fold) on HaCaT cells (Pelin et al., 2016b). The impact of PITX on Caco-2 monolayer integrity has already been evidenced but at lower concentrations: a 40% decrease of TEER at 36 ng/mL (13.5 nM) after 2 h exposure reaching 50% decrease at 3.6 ng/mL (1.35 nM) and even 90% decrease at 36 ng/mL (13.5 nM) after 10 h exposure (Fernández et al., 2013). In fact, the low effect reported on Caco-2 monolayer compared to the high sensitivity of other cells, included non-differentiated Caco-2 cells, is likely to be due to the presence of the Na<sup>+</sup>/K<sup>+</sup> ATPase only at the basolateral membrane of differentiated Caco-2 cells (Aiba et al., 2005; Giannella et al., 1993; Raffaniello et al., 1992). As the Caco-2 monolayer integrity was decreased only after a long-time exposure (24 h), without any effect after a short time treatment (4 h), we suggest that PITX reached its Na<sup>+</sup>/K<sup>+</sup>-ATPase target only after crossing the monolayer (whether through para or transcellular pathway), thus affecting the monolayer after a longer time exposure. The difference of response observed in this study compared to Fernandez et al (2013) is likely due to the variability of Caco-2 monolayers permeability. The comparison of TEER values would have helped to confirm this



hypothesis but these data were not provided in Fernandez et al (2013). Nevertheless, it could not be excluded that PITX reacted also through other pathways such as membrane conductive pathway for H<sup>+</sup> and elevation of intracellular Ca<sup>2+</sup> as depicted in different cell types (Vale et al., 2006; Wu, 2009) or in *ex vivo* rat colon samples (Scheiner-Bobis et al., 1994). Even if we intended to compare the intestinal crossing of the pure toxins, neither LC-MS/MS analytical method nor cell based assays were able to detect the very low maximal amounts of toxin tested on differentiated Caco-2 cells: for PITX, LOQ and LOD values for analytics = 40 and 20 ng/mL respectively and IC<sub>50</sub> around 1 ng/mL on Neuro2A cells at 24 h (data not shown). It must be highlighted that we observed a shift in toxicity between the MTT assay performed on 96-well plates and the permeability tests done on inserts. We suggested above that the effect of PITX (and probably OVTXs) on differentiated Caco2 cells could be observed only when the toxin reached the Na<sup>+</sup>/K<sup>+</sup>ATPase mainly located on the basal side. If this is true, we expect that better conditions for the toxin to reach its target would be present through the basolateral medium of inserts compared to the plastic support of 96 well plates.

In this study, PITX and analogs were shown to induce an inflammatory response of human intestinal cells. The IL-8 release was observed with 2 ng/mL (0.75 nM) PITX but also, more moderately, with OVTX- a and -d (around 1.5 and 2.5 fold respectively) and with *Ostreopsis cf. ovata* crude extracts that contained several OVTXs. However, while a decrease of IL-8 release was observed at higher and cytotoxic concentrations of PITX (above 12.5 ng/mL), this was not the case for OVTX-a and -d (up to 20 ng/mL). For both OVTXs, the increase of IL-8 release was dose-dependent prior to a decrease unlinked to any sign of cytotoxicity. The peak of IL-8 release was observed at a lower concentration of OVTX-d (1.25 ng/mL = 0.47 nM) compared to OVTX-a (5 ng/mL = 1.89 nM), although IL-8 reached a higher level (around 2 fold) with OVTX-a. However, we cannot explain why a decrease of IL-8 release was observed with higher concentrations of OVTX-a and -d without inducing any cytotoxicity. These toxins may have both an inducing effect of cytokine production at low concentrations and a suppressive one at higher concentrations, which suggests different cellular targets depending on toxin concentration. *In vitro* results from the literature showed that PITX induced the release of

cytokines by HaCaT keratinocytes (Pelin et al., 2016a): for IL-8, a 2.1 fold increase was observed with 0.026 ng/mL (10 pM) PITX exposure for 24 h. The inflammation response has been shown to involve the NFkB and P38 MAPK signaling pathways in immune cells (Crinelli et al., 2012). It has been shown that PITX interacts with Na<sup>+</sup>/K<sup>+</sup>-ATPase through a saturable and reversible binding to HaCaT cells (Pelin et al., 2018). Therefore, a difference of OVTX binding to Na<sup>+</sup>/K<sup>+</sup>-ATPase can be suggested to explain why OVTXs induced some inflammation with non-toxic low concentrations compared to PITX. Surprisingly, in *in vivo* studies with oral administration of PITX, no inflammation was observed along the intestine (Sosa et al., 2009) but it occurred in the non-glandular stomach. However, enteritis with infiltration of hemocytes was detected in mussels exposed to *Ostreopsis cf. ovata* (Carella et al., 2015) and inflammation of the spleen was induced by PITX after repeated intraperitoneal injections in mice (Ito et al., 1996). The recent publications on PITX oral toxicity in mice ((Boente-Juncal et al., 2020a; Boente-Juncal et al., 2020b) concluded that PITX induced abdominal swelling and the presence of gas and mucus in the stomach and intestines. Although ultrastructural modifications were observed on the stomach epithelium, they did not provide any histological information that could established if PITX could generate intestinal inflammation as suggested by our results. Unfortunately, the only *in vivo* data with an extract of OVTXs did not show much lesions in the gastrointestinal tract but the oral route of administration was not tested (Poli et al., 2018).

## 5 Conclusion

This is the first study investigating the *in vitro* toxicity of OVTX-d, including also a comparison with OVTX-a and PITX. No ranking on the cytotoxicity test can be proposed but our results showed that both OVTX-a and-d induced an inflammatory response of differentiated Caco-2 cells, although OVTX-a was slightly more potent than OVTX-d. OVTX-a also affected the monolayer integrity. For these two endpoints, PITX showed a more toxic potential compared to OVTX-a and -d.

**Funding:** This project was funded by the project OCEAN-15 funded by the ANR-15-CE35-0002-04.

**Author Contributions:** Conceptualization; R.L., D.R., Z.A. and V.F. Formal analysis; M-P.G., R.L., F.H. and D.R. Funding acquisition; Z.A., E.T., O.T. and V.F. Investigation; M-P. G., R.L., L.M. and F.H. Methodology; R.L., F.H., D.R., and V.F. Project administration; Z.A., E.T, O.T. and V.F. Supervision; D.R., Z.A. and V.F. Validation; R.L. Visualization; M-P.G., R.L. and O.T. Roles/Writing - original and revised draft; R.L., M-P. G. and V.F. Writing - review & editing. D.R, Z.A., E.T., O.T. and V.F.

**Conflicts of Interest:** The authors declare no conflict of interest.

**Acknowledgment:** We would like to thank Pr Rodolphe Lemée (Laboratoire Océanographique de Villefranche/Mer, France) for providing the *Ostreopsis cf. ovata* strains and advices.

## 6 References

- Aiba, T., Ishida, K., Yoshinaga, M., Okuno, M., Hashimoto, Y., 2005. Pharmacokinetic Characterization of Transcellular Transport and Drug Interaction of Digoxin in Caco-2 Cell Monolayers. *Biological and Pharmaceutical Bulletin* 28, 114-119.
- Aligizaki, K., Katikou, P., Nikolaidis, G., Panou, A., 2008. First episode of shellfish contamination by palytoxin-like compounds from *Ostreopsis* species (Aegean Sea, Greece). *Toxicon* 51, 418-427.
- Amzil, Z., Sibat, M., Chomerat, N., Grosseil, H., Marco-Miralles, F., Lemee, R., Nezan, E., Séchet, V., 2012. Ovatoxin-a and palytoxin accumulation in seafood in relation to *Ostreopsis cf. ovata* blooms on the French Mediterranean coast. *Mar Drugs* 10, 477-496.
- Bates, N., Morrison, C., Flaig, L., Turner, A.D., 2020. Paralytic shellfish poisoning and palytoxin poisoning in dogs. *Veterinary Record* 187, e46.
- Biré, R., Trottereau, S., Lemée, R., Oregioni, D., Delpont, C., Krys, S., Guérin, T., 2015. Hunt for Palytoxins in a Wide Variety of Marine Organisms Harvested in 2010 on the French Mediterranean Coast. *Mar Drugs* 13, 5425-5446.
- Boente-Juncal, A., Raposo-García, S., Vale, C., Louzao, M.C., Otero, P., Botana, L.M., 2020a. In Vivo Evaluation of the Chronic Oral Toxicity of the Marine Toxin Palytoxin. *Toxins* 12.
- Boente-Juncal, A., Vale, C., Camiña, M., Cifuentes, J.M., Vieytes, M.R., Botana, L.M., 2020b. Reevaluation of the acute toxicity of palytoxin in mice: Determination of lethal dose 50 (LD50) and No-observed-adverse-effect level (NOAEL). *Toxicon* 177, 16-24.
- Brissard, C., Herrenknecht, C., Séchet, V., Hervé, F., Pisapia, F., Harcouet, J., Lemée, R., Chomérat, N., Hess, P., Amzil, Z., 2014. Complex toxin profile of French Mediterranean *Ostreopsis cf. ovata* strains, seafood accumulation and ovatoxins prepurification. *Marine Drugs* 12, 2851-2876.
- Brissard, C., Hervé, F., Sibat, M., Séchet, V., Hess, P., Amzil, Z., Herrenknecht, C., 2015. Characterization of ovatoxin-h, a new ovatoxin analog, and evaluation of chromatographic columns for ovatoxin analysis and purification. *Journal of Chromatography A* 1388, 87-101.
- Calon, T., Sinno-Tellier, S., de Haro, L., Bloch, J., 2019. Exposition à la palytoxine des personnes manipulant des coraux mous d'aquarium d'eau de mer : étude des cas rapportés au réseau des Centres antipoison de 2000 à 2017. *Toxicologie Analytique & Clinique* 31, 64-76.

Carella, F., Sardo, A., Mangoni, O., Di Cioccio, D., Urciuolo, G., De Vico, G., Zingone, A., 2015. Quantitative histopathology of the Mediterranean mussel (*Mytilus galloprovincialis* L.) exposed to the harmful dinoflagellate *Ostreopsis cf. ovata*. *Journal of Invertebrate Pathology* 127, 130-140.

Ciminiello, P., Dell'Aversano, C., Dello Iacovo, E., Fattorusso, E., Forino, M., Grauso, L., Tartaglione, L., Guerrini, F., Pistocchi, R., 2010. Complex palytoxin-like profile of *Ostreopsis ovata*. Identification of four new ovatoxins by high-resolution liquid chromatography/mass spectrometry. *Rapid communications in mass spectrometry* : RCM 24, 2735-2744.

Ciminiello, P., Dell'Aversano, C., Dello Iacovo, E., Fattorusso, E., Forino, M., Grauso, L., Tartaglione, L., 2012a. Stereochemical Studies on Ovatoxin-a. *Chemistry – A European Journal* 18, 16836-16843.

Ciminiello, P., Dell'Aversano, C., Iacovo, E.D., Fattorusso, E., Forino, M., Tartaglione, L., Battocchi, C., Crinelli, R., Carloni, E., Magnani, M., Penna, A., 2012b. Unique toxin profile of a Mediterranean *Ostreopsis cf. ovata* strain: HR LC-MS(n) characterization of ovatoxin-f, a new palytoxin congener. *Chem Res Toxicol* 25, 1243-1252.

Ciminiello, P., Dell'Aversano, C., Dello Iacovo, E., Fattorusso, E., Forino, M., Grauso, L., Tartaglione, L., 2012c. High Resolution LC-MSn Fragmentation Pattern of Palytoxin as Template to Gain New Insights into Ovatoxin-a Structure. The Key Role of Calcium in MS Behavior of Palytoxins. *Journal of The American Society for Mass Spectrometry* 23, 952-963.

Ciminiello, P., Dell'Aversano, C., Dello Iacovo, E., Fattorusso, E., Forino, M., Grauso, L., Tartaglione, L., Guerrini, F., Pezzolesi, L., Pistocchi, R., Vanucci, S., 2012d. Isolation and Structure Elucidation of Ovatoxin-a, the Major Toxin Produced by *Ostreopsis ovata*. *Journal of the American Chemical Society* 134, 1869-1875.

Crinelli, R., Carloni, E., Giacomini, E., Penna, A., Dominici, S., Battocchi, C., Ciminiello, P., Dell'Aversano, C., Fattorusso, E., Forino, M., Tartaglione, L., Magnani, M., 2012. Palytoxin and an *Ostreopsis* toxin extract increase the levels of mRNAs encoding inflammation-related proteins in human macrophages via p38 MAPK and NF- $\kappa$ B. *PloS one* 7, e38139.

Farooq, A.V., Gibbons, A.G., Council, M.D., Harocopos, G.J., Holland, S., Judelson, J., Shoss, B.L., Schmidt, E.J., Md Noh, U.K., D'Angelo, A., Chundury, R.V., Judelson, R., Perez, V.L., Huang, A.J.W., 2017. Corneal Toxicity Associated With Aquarium Coral Palytoxin. *American journal of ophthalmology* 174, 119-125.

Fernández, D.A., Louzao, M.C., Vilariño, N., Espiña, B., Fraga, M., Vieytes, M.R., Román, A., Poli, M., Botana, L.M., 2013. The kinetic, mechanistic and cytomorphological effects of palytoxin in human intestinal cells (Caco-2) explain its lower-than-parenteral oral toxicity. *The FEBS Journal* 280, 3906-3919.

García-Altres, M., Tartaglione, L., Dell'Aversano, C., Carnicer, O., de la Iglesia, P., Forino, M., Diogène, J., Ciminiello, P., 2015. The novel ovatoxin-g and isobaric palytoxin (so far referred to as putative palytoxin) from *Ostreopsis cf. ovata* (NW Mediterranean Sea): structural insights by LC-high resolution MS(n). *Analytical and bioanalytical chemistry* 407, 1191-1204.

Gémin, M.P., Réveillon, D., Hervé, F., Pavaux, A.S., Tharaud, M., Séchet, V., Bertrand, S., Lemée, R., Amzil, Z., 2020. Toxin content of *Ostreopsis cf. ovata* depends on bloom phases, depth and macroalgal substrate in the NW Mediterranean Sea. *Harmful Algae* 92, 101727.

Giannella, R.A., Orłowski, J., Jump, M.L., Lingrel, J.B., 1993. Na(+)-K(+)-ATPase gene expression in rat intestine and Caco-2 cells: response to thyroid hormone. *The American journal of physiology* 265, G775-782.

Guerrini, F., Pezzolesi, L., Feller, A., Riccardi, M., Ciminiello, P., Dell'Aversano, C., Tartaglione, L., Dello Iacovo, E., Fattorusso, E., Forino, M., Pistocchi, R., 2010. Comparative growth and toxin profile of cultured *Ostreopsis ovata* from the Tyrrhenian and Adriatic Seas. *Toxicon* 55, 211-220.

Guillard, R.R.L., 1975. The culture of phytoplankton for feeding marine invertebrates. *The Culture of Marine Invertebrates Animals*, 29-60.

Habermann, E., 1989. Palytoxin acts through Na<sup>+</sup>,K<sup>+</sup>-ATPase. *Toxicon* 27, 1171-1187.

Hahne, H., Pachl, F., Ruprecht, B., Maier, S., Klaeger, S., Helm, D., Médard, G., Wilm, M., Lemeer, S., Kuster, B., 2013. DMSO enhances electrospray response, boosting sensitivity of proteomic experiments. *Nature methods* 10.

Hall, C., Levy, D., Sattler, S., 2015. A Case of Palytoxin Poisoning in a Home Aquarium Enthusiast and His Family. *Case Reports in Emergency Medicine* 2015, 621815.

Ito, E., Ohkusu, M., Yasumoto, T., 1996. Intestinal injuries caused by experimental palytoxicosis in mice. *Toxicon* 34, 643-652.

Ito, E., Yasumoto, T., 2009. Toxicological studies on palytoxin and ostreocin-D administered to mice by three different routes. *Toxicon* 54, 244-251.

Jauzein, C., Couet, D., Blasco, T., Lemée, R., 2017. Uptake of dissolved inorganic and organic nitrogen by the benthic toxic dinoflagellate *Ostreopsis cf. ovata*. *Harmful algae* 65, 9-18.

Kermarec, F., Dor, F., Armengaud, A., Charlet, F., Kantin, R., Sauzade, D., de Haro, L., 2008. Health risks related to *Ostreopsis ovata* in recreational waters. *Environnement, Risques & Santé* 7, 357-363.

Louzao, M.C., Ares, I.R., Cagide, E., 2008. Marine toxins and the cytoskeleton: a new view of palytoxin toxicity. *The FEBS Journal* 275, 6067-6074.

Patocka, J., Nepovimova, E., Wu, Q., Kuca, K., 2018. Palytoxin congeners. *Archives of Toxicology* 92, 143-156.

Pavaux, A.-S., Ternon, E., Dufour, L., Marro, S., Gémin, M.-P., Thomas, O.P., Lemée, R., 2020. Efficient, fast and inexpensive bioassay to monitor benthic microalgae toxicity: Application to *Ostreopsis* species. *Aquatic Toxicology* 223, 105485.

Pelin, M., Florio, C., Ponti, C., Lucafò, M., Gibellini, D., Tubaro, A., Sosa, S., 2016a. Pro-inflammatory effects of palytoxin: an in vitro study on human keratinocytes and inflammatory cells. *Toxicology Research* 5, 1172-1181.

Pelin, M., Forino, M., Brovedani, V., Tartaglione, L., Dell'Aversano, C., Pistocchi, R., Poli, M., Sosa, S., Florio, C., Ciminiello, P., Tubaro, A., 2016b. Ovatoxin-a, A Palytoxin Analogue Isolated from *Ostreopsis cf. ovata* Fukuyo: Cytotoxic Activity and ELISA Detection. *Environmental Science & Technology* 50, 1544-1551.

Pelin, M., Sosa, S., Brovedani, V., Fusco, L., Poli, M., Tubaro, A., 2018. A Novel Sensitive Cell-Based Immunoenzymatic Assay for Palytoxin Quantitation in Mussels. *Toxins* 10.

Pelin, M., Sosa, S., Della Loggia, R., Poli, M., Tubaro, A., Decorti, G., Florio, C., 2012. The cytotoxic effect of palytoxin on Caco-2 cells hinders their use for in vitro absorption studies. *Food and Chemical Toxicology* 50, 206-211.

Pelin, M., Stocco, G., Florio, C., Sosa, S., Tubaro, A., 2020. In Vitro Cell Sensitivity to Palytoxin Correlates with High Gene Expression of the Na(+)/K(+)-ATPase  $\beta$ 2 Subunit Isoform. *International journal of molecular sciences* 21.

Poli, M., Ruiz-Olvera, P., Nalca, A., Ruiz, S., Livingston, V., Frick, O., Dyer, D., Schellhase, C., Raymond, J., Kulis, D., Anderson, D., McGrath, S., Deeds, J., 2018. Toxicity and pathophysiology of palytoxin congeners after intraperitoneal and aerosol administration in rats. *Toxicon* 150, 235-250.

Raffaniello, R.D., Lee, S.Y., Teichberg, S., Wapnir, R.A., 1992. Distinct mechanisms of zinc uptake at the apical and basolateral membranes of caco-2 cells. *Journal of cellular physiology* 152, 356-361.

Reale, O., Huguet, A., Fessard, V., 2020. Co-culture model of Caco-2/HT29-MTX cells: A promising tool for investigation of phycotoxins toxicity on the intestinal barrier. *Chemosphere*, 128497.

Satoh, E., Ishii, T., Nishimura, M., 2003. Palytoxin-induced increase in cytosolic-free Ca(2+) in mouse spleen cells. *European journal of pharmacology* 465, 9-13.

Scheiner-Bobis, G., Meyer zu Heringdorf, D., Christ, M., Habermann, E., 1994. Palytoxin induces K+ efflux from yeast cells expressing the mammalian sodium pump. *Molecular Pharmacology* 45, 1132.

Schulz, M., Łoś, A., Szabelak, A., Strachecka, A., 2019. Inhalation poisoning with palytoxin from aquarium coral: case description and safety advice. *Archives of Industrial Hygiene and Toxicology* 70, 14-17.

Séchet, V., Sibat, M., Chomérat, N., Nézan, E., Gossel, H., Lehebel-Peron, J.-B., Jauffrais, T., Ganzin, N., Marco-Miralles, F., Lemée, R., Amzil, Z., 2012. *Ostreopsis cf. ovata* in the French Mediterranean Coast: Molecular Characterisation and Toxin Profile. *Cryptogamie, Algologie* 33, 89-98.

Soliño, L., García-Altres, M., Godinho, L., Costa, P.R., 2020. Toxin profile of *Ostreopsis cf. ovata* from Portuguese continental coast and Selvagens Islands (Madeira, Portugal). *Toxicon* 181, 91-101.

Sosa, S., Del Favero, G., De Bortoli, M., Vita, F., Soranzo, M.R., Beltramo, D., Ardizzone, M., Tubaro, A., 2009. Palytoxin toxicity after acute oral administration in mice. *Toxicology Letters* 191, 253-259.

Tartaglione, L., Dello Iacovo, E., Mazzeo, A., Casabianca, S., Ciminiello, P., Penna, A., Dell'Aversano, C., 2017. Variability in Toxin Profiles of the Mediterranean *Ostreopsis cf. ovata* and in Structural Features of the Produced Ovatoxins. *Environmental Science & Technology* 51, 13920-13928.

Tartaglione, L., Mazzeo, A., Dell'Aversano, C., Forino, M., Giussani, V., Capellacci, S., Penna, A., Asnaghi, V., Faimali, M., Chiantore, M., Yasumoto, T., Ciminiello, P., 2016. Chemical, molecular, and eco-toxicological investigation of *Ostreopsis* sp. from Cyprus Island: structural insights into four new ovatoxins by LC-HRMS/MS. *Analytical and bioanalytical chemistry* 408, 915-932.

Tubaro, A., Durando, P., Del Favero, G., Ansaldi, F., Icardi, G., Deeds, J.R., Sosa, S., 2011. Case definitions for human poisonings postulated to palytoxins exposure. *Toxicon* 57, 478-495.

Vale, C., Alfonso, A., Suñol, C., Vieytes, M.R., Botana, L.M., 2006. Modulation of calcium entry and glutamate release in cultured cerebellar granule cells by palytoxin. *Journal of neuroscience research* 83, 1393-1406.

Valverde, I., Lago, J., Vieites, J.M., Cabado, A.G., 2008. In vitro approaches to evaluate palytoxin-induced toxicity and cell death in intestinal cells. *Journal of Applied Toxicology* 28, 294-302.

Vila, M., Abós-Herràndiz, R., Isern-Fontanet, J., Àlvarez, J., Berdalet, E., 2016. Establishing the link between *Ostreopsis cf. ovata* blooms and human health impacts using ecology and epidemiology. *Scientia Marina* 80, 107–115.

Wiles, J.S., Vick, J.A., Christensen, M.K., 1974. Toxicological evaluation of palytoxin in several animal species. *Toxicon* 12, 427-433.

Wonneberger, W., Claesson, M., Zetterberg, M., 2020. Corneal perforation due to palytoxin exposure of domestic zoanthid corals. *Acta Ophthalmologica* n/a.

Wu, C.H., 2009. Palytoxin: Membrane mechanisms of action. *Toxicon* 54, 1183-1189.

Figure 1: Chemical structures of palytoxin and ovatoxin-a and -d.

Figure 2: Cytotoxicity (MTT assay) of MCCV54 and MCCV55 crude extracts on differentiated Caco-2 cells after 24 h treatment. Mean  $\pm$  standard deviation of 4 independent experiments.

Figure 3: Cytotoxicity (MTT assay) of PITX and OVTX-a and -d on differentiated Caco-2 cells after 24 h treatment. Mean  $\pm$  standard deviation of 4 independent experiments.

Figure 4: IL-8 release of differentiated Caco-2 cells following 24 h treatment with MCCV54 and 55 crude extracts. Mean  $\pm$  standard deviation of 3 independent experiments. Positive control = TNF $\alpha$  100 ng/mL; \* = value significantly different from the solvent control, P <0.05

Figure 5: IL-8 release of differentiated Caco-2 cells following 24 h treatment with PITX and OVTX-a and -d. Mean  $\pm$  standard deviation of 4 independent experiments. Positive control = TNF $\alpha$  100 ng/mL; \* = value significantly different from the solvent control, P <0.05

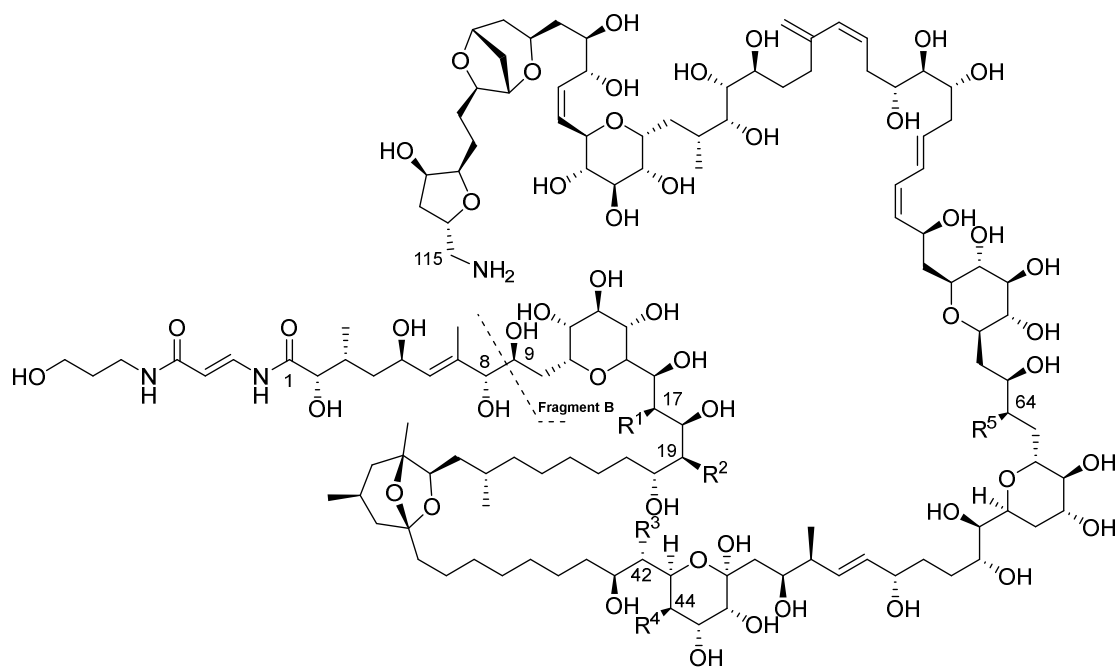
Figure 6: TEER (% compared to the solvent control) after 4 and 24 h treatment of differentiated Caco-2 cells with MCCV54 (A) and MCCV55 (B) crude extracts. Mean  $\pm$  standard deviation for 2 to 4 independent experiments (except 1.21 ng PITX eq./mL for MCCV55 at 4 h treatment that was done only once). The solvent control was set to 100%.

Figure 7: LY Papp after 4 and 24 h treatment of differentiated Caco-2 cells with MCCV54 (A) and MCCV55 (B) crude extracts. Mean  $\pm$  standard deviation for 2 to 4 independent experiments. \* = value significantly different from the solvent control, P <0.05

Figure 8: TEER (% compared to the solvent control) after 4 and 24 h treatment of differentiated Caco-2 cells with PITX (A) OVTX-a (B) and OVTX-d (C). Mean  $\pm$  standard deviation for 2 to 4 independent experiments. The solvent control was set to 100%. \* = value significantly different from the solvent control, P <0.05

Figure 9: LY Papp after 4 and 24 h treatment of differentiated Caco-2 cells with PITX (A) OVTX-a (B) and OVTX-d (C). Mean standard deviation for 2 to 4 independent experiments. Mean  $\pm$  standard deviation for 2 to 4 independent experiments. \* = value significantly different from the solvent control, P <0.05





Compound	Formula	<i>m/z</i>	R <sup>1</sup>	R <sup>2</sup>	R <sup>3</sup>	R <sup>4</sup>	R <sup>5</sup>	Reference
Palytoxin	C <sub>129</sub> H <sub>223</sub> N <sub>3</sub> O <sub>54</sub>	2678.48	OH	OH	H	OH	OH	Uemura et al. 1981a, b
Ovatoxin-a	C <sub>129</sub> H <sub>223</sub> N <sub>3</sub> O <sub>52</sub>	2646.49	H	OH	OH	H	H	Ciminiello et al. 2012a, b
Ovatoxin-d	C <sub>129</sub> H <sub>223</sub> N <sub>3</sub> O <sub>53</sub>	2662.48	same as OVTX-a + O in fragment B					Ciminiello et al. 2010

Figure 1

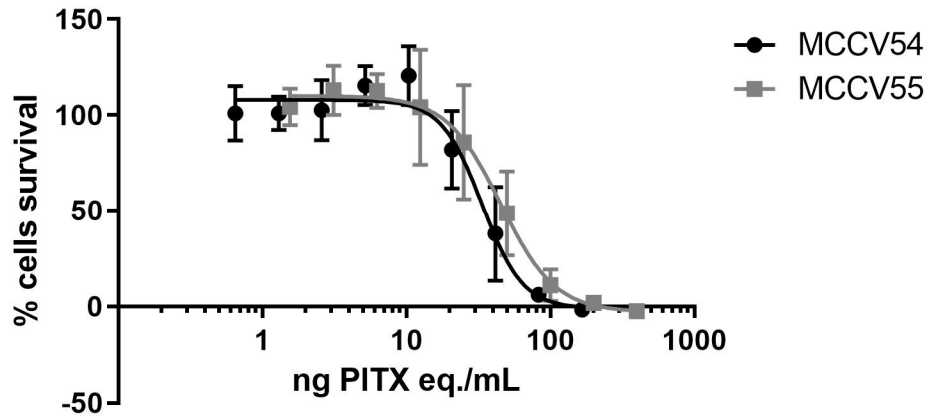


Figure 2

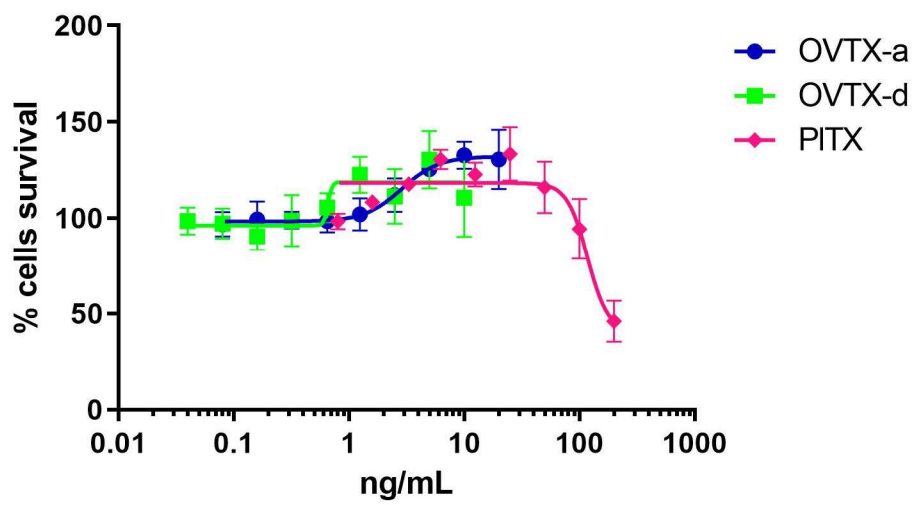


Figure 3

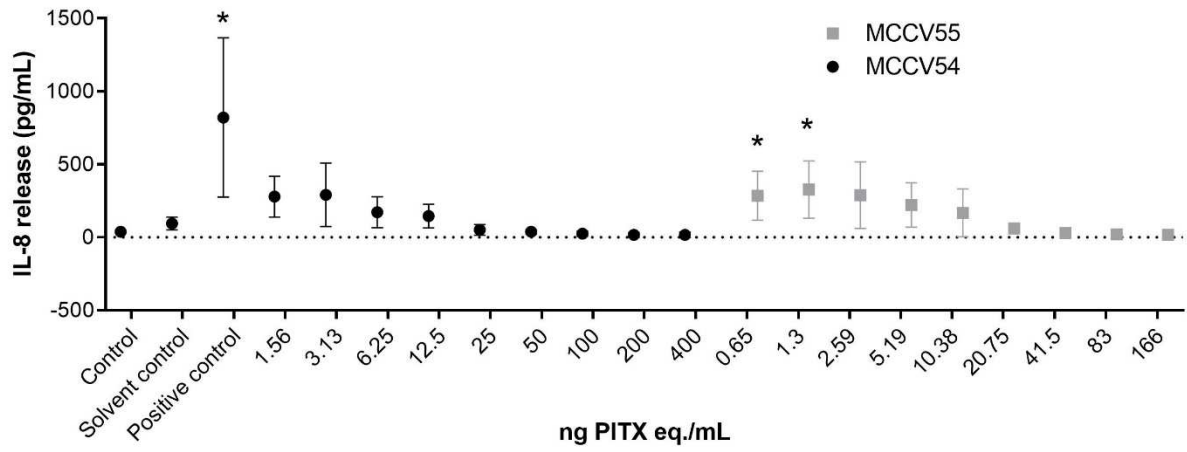


Figure 4

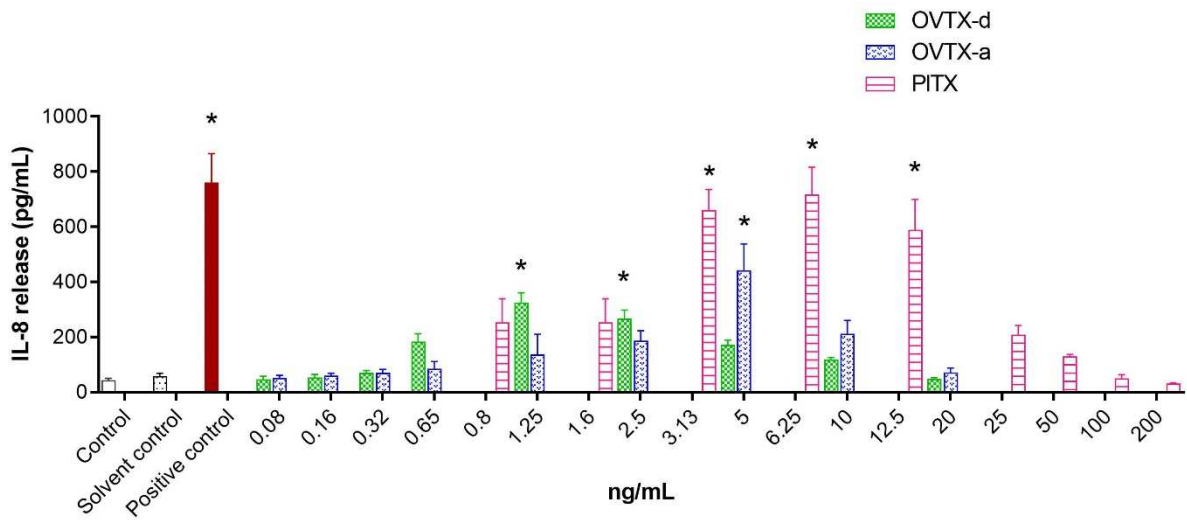


Figure 5

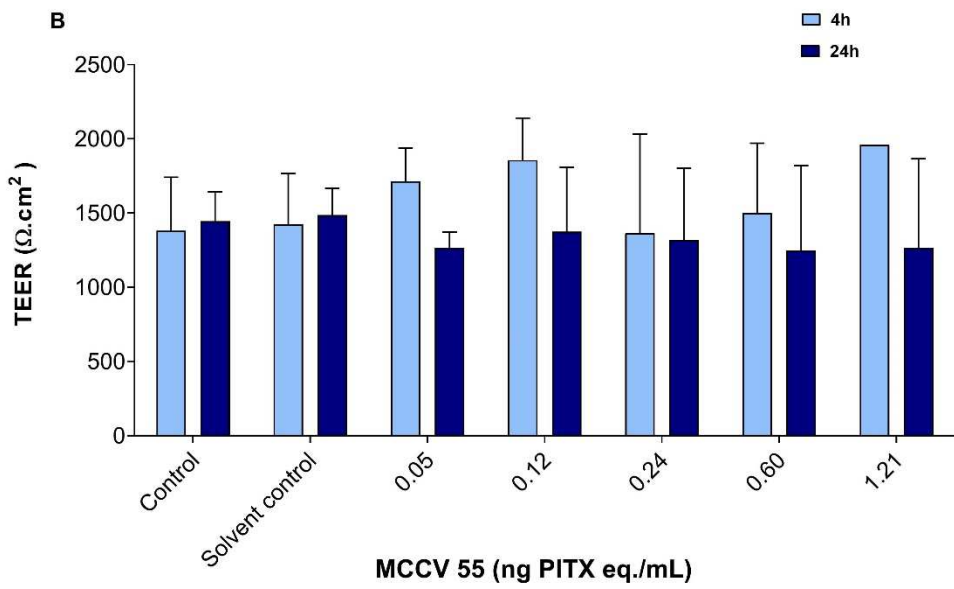
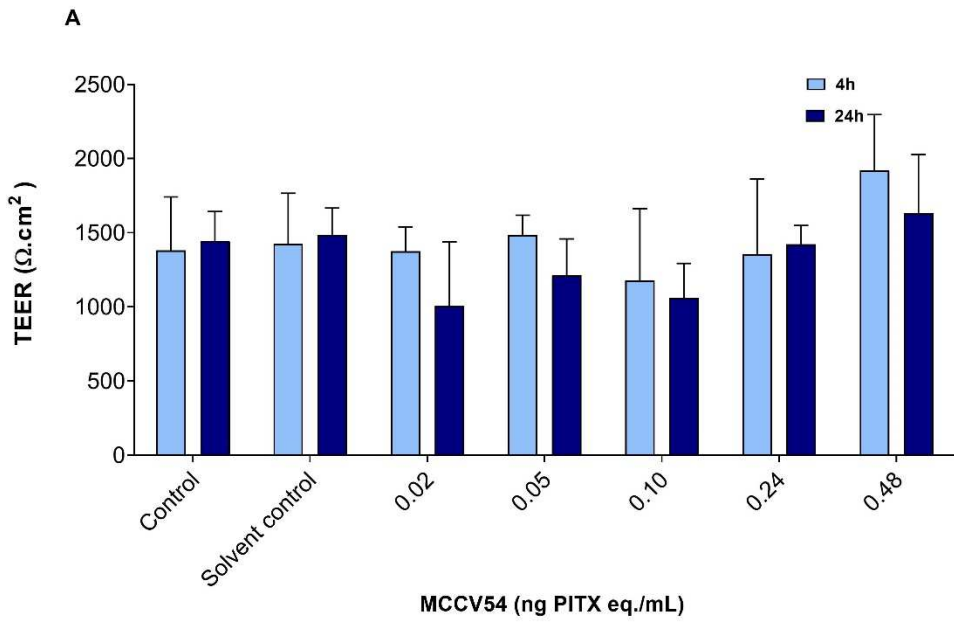


Figure 6

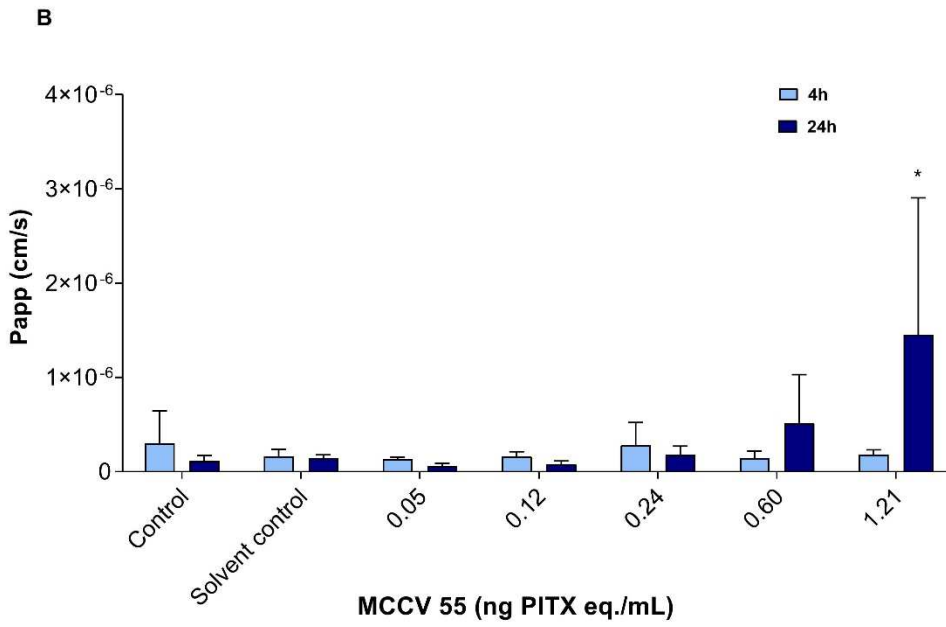
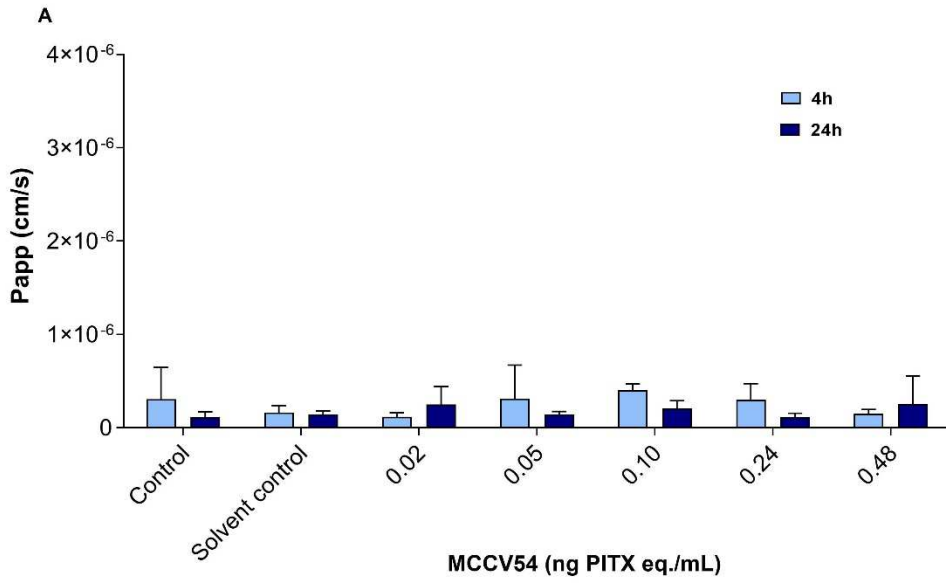


Figure 7

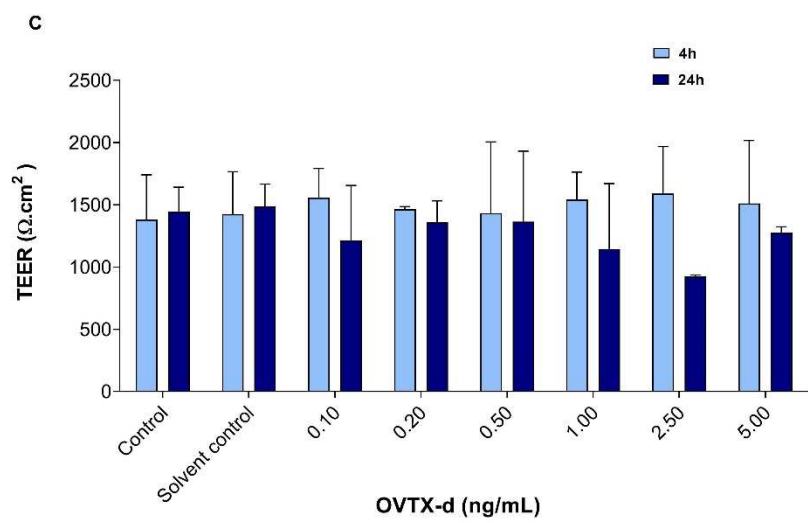
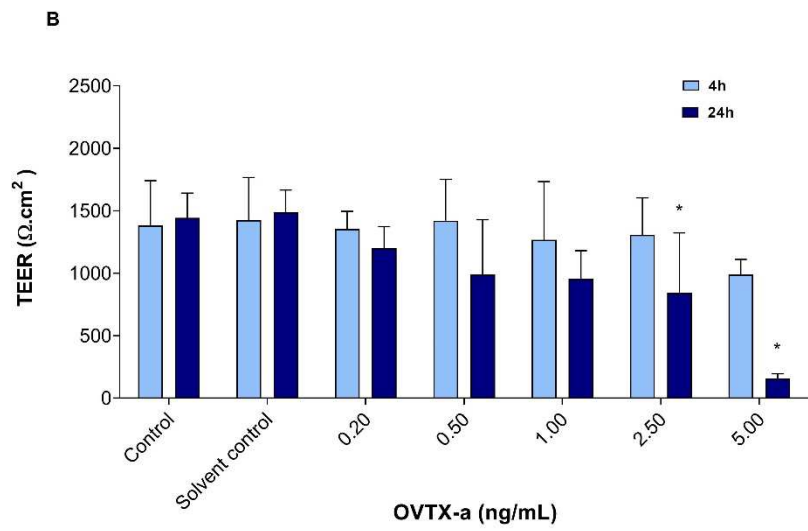
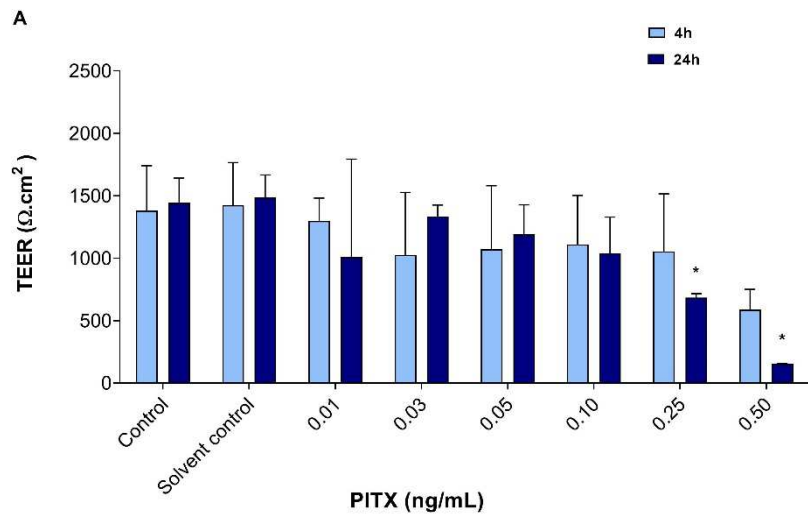


Figure 8

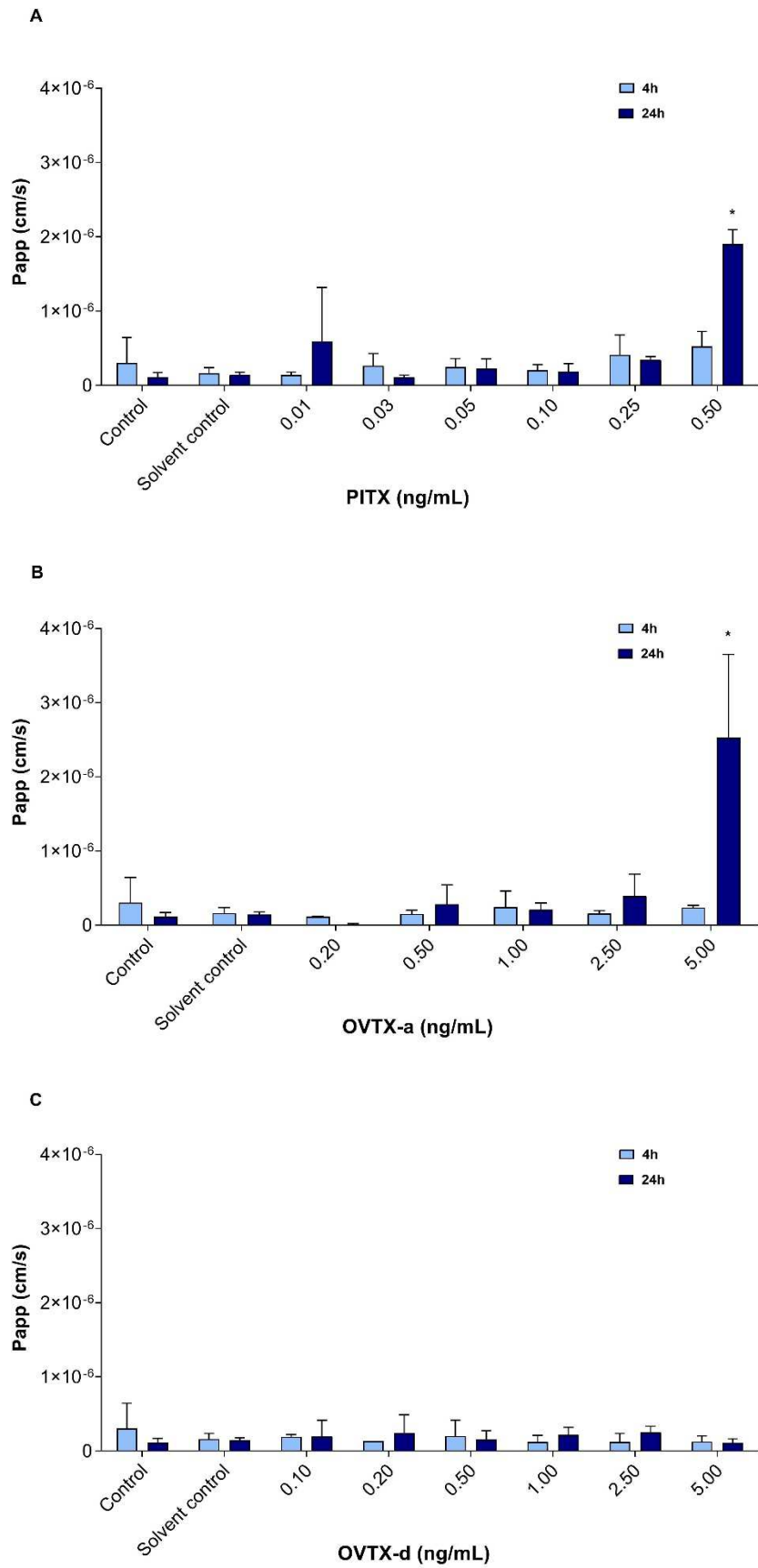


Figure 9

		Iso-PITX	OVTX-a	OVTX-b	OVTX-c	OVTX-d	OVTX-e	OVTX-f	Total
<b>MCCV54 extract</b>	ng PITX eq./mL	< LOD	4,900	2,700	180	320	250	< LOD	8,300
	%	-	58	33	2.2	3.8	3	-	100
<b>MCCV55 extract</b>	ng PITX eq./mL	< LOD	18,000	< LOD	< LOD	900	1,200	< LOD	20,000
	%	-	89	-	-	4.5	6.2	-	100



	<b>MTT</b>	<b>IL8</b>	<b>TEER</b>	<b>Papp LY</b>
<b>MCCV54</b>	IC50 = 45.23 ng PITX eq./mL	Maximum at 1.3 ng PITX eq./mL	No effect up to 0.48 ng PITX eq./mL	No effect up to 0.48 ng PITX eq./mL
<b>MCCV55</b>	IC50 = 33.53 ng PITX eq./mL	Maximum at 3.13 ng PITX eq./mL	No effect up to 1.21 ng PITX eq./mL	Increase at 1.21 ng PITX eq./mL
<b>PITX</b>	IC50 around 200 ng/mL	Maximum at 6.25 ng/mL	Decrease at 0.25 and 0.5 ng/mL	Increase at 0.5 ng/mL
<b>OVTX-a</b>	No toxicity up to 20 ng/mL	Maximum at 5 ng/mL	Decrease at 2.5 and 5 ng/mL	Increase at 5 ng/mL
<b>OVTX-d</b>	No toxicity up to 20 ng/mL	Maximum at 1.25 ng/mL	No effect up to 5 ng/mL	No effect up to 5 ng/mL